JOURNAL OF ADVANCED DIELECTRICS
Vol. 8, No. 3 (2018) 1850018 (14 pages)

DOI: 10.1142/S2010135X18500182

World Scientific
www.worldscientific.com

Electric memory effects in styrene-butadiene rubber, containing electric inclusions of highly aromatic oil

Ricardo Raúl Mocellini, Federico Guillermo Bonifacich, Fernando Daniel Lambri, Mariel Antonella Lambri, Griselda Irene Zelada and Osvaldo Agustín Lambri*
CONICET-UNR, Laboratorio de Materiales, Escuela de Ingeniería Eléctrica
Centro de Tecnología e Investigación Eléctrica
Facultad de Ciencias Exactas, Ingeniería y Agrimensura
Avda. Pellegrini 250, Rosario 2000, Argentina
*olambri@fceia.unr.edu.ar

Received 5 March 2018; Revised 25 May 2018; Accepted 28 May 2018; Published 5 July 2018

It was determined that samples of styrene-butadiene rubber (SBR), containing highly aromatic oil, exhibit memory effects giving rise to dynamic elastic modulus, damping and internal stresses degree which can be tailored depending on the applied electric field strength. The capability and stability of the interaction process between aligned neighbor dipoles for exhibiting a memory effect, once the aligning electric field was removed are studied. It is determined that depending on the spatial arrangement and the amount of electric charge of the dipoles, this interaction is able to promote a memory effect which keeps the alignment between them. This electrostatic interaction plays the role of a counteracting effect for keeping the alignment, which was called electroelasticity. The results from the developed model were applied successfully to SBR composite samples for explaining the memory effects recorded from dynamic mechanical analysis (DMA) measurements under electric field. In addition, the model of the electric inclusion based on the inclusion theory for continuous media, was applied to determine the degree of internal stresses in the dielectric composite material due to the external applied electric field. In addition, from the coupling between the model developed here and simple issues related to the mechanical properties of composite materials, a procedure for determining the maximum possible gap between the electric dipoles in composite dielectric materials is also shown.

Keywords: Modeling; memory effect; dynamic mechanical analysis; electric interaction; polymer matrix composite with electric inclusions.

1. Introduction

In a recent work, a mesoscopic description of magnetite-filled polymer composite materials has been performed in the continuous media by considering the interaction between magnetic and mechanical forces.[1] Magnetomechanical interaction is caused by both the magnetic forces between two adjacent particles trying to align them and an elastic deformation of the matrix which is counteracting. Theoretical predictions are successfully explained in a qualitative mode where the memory effect in magnetite-filled polypropylene composite is under the application of a direct magnetic field.[1] As it was also highlighted in Ref. 1, the mathematical formalism developed can be extrapolated to the case of electric materials.

In addition, the electrostriction effect was studied by means of the theory of inclusions,[2,3] giving rise to the so-called electric inclusion model.[4–6] The model allows determining the behavior of internal stresses promoted by the electrostriction phenomenon by monitoring the behavior of the misfit coefficient and the transfer process of elastic energy.[4–6] In fact, the electric inclusion model considers that applying an electric field to a dielectric material leads to the stretching of dipoles giving rise to the appearance of inclusions. They promote the development of internal stresses in the dielectric material, whose electromechanical equilibrium condition is determined from the inclusion formalism for continuous media.[4–6]

In the present paper, it was discovered that styrene-butadiene rubber (SBR), containing highly aromatic oil (HAO), under electric field, transforms to a composite involving electric inclusions; which exhibits memory effects. It gives rise to dynamic elastic modulus, damping and internal stresses degree which can be controlled depending on the applied electric field strength. The driving force giving rise to the memory behavior is related to the retention of electric dipoles in the HAO. Therefore, we have modified and adapted the model for describing memory effects in magnetite-filled polypropylene composites[1] to explain the electric memory behavior which takes place in HAO. The results from dynamic mechanical analysis (DMA) under electric field on SBR containing HAO were correlated with the behavior of the viscosity under electric field on HAO.

The model of the electric inclusion based on the inclusion theory for continuous media was also applied to determine

the degree of internal stresses in the dielectric composite due to the external applied electric field.

Moreover, from the coupling between the theoretical model developed here for memory and simple issues related to the mechanical properties of composite materials, a procedure for determining the maximum possible gap between the electric dipoles in the composites dielectric is also shown.

2. Experimental

2.1. *Materials*

Rubber samples were prepared with raw SBR (styrene-butadiene rubber, cold emulsion polymerization, 23.5% bound styrene). Two different grades of SBR were used: SBR 1502 (typical Mn 140000 Da, Mw 500000 Da) and SBR 1712 (typical Mn 210000 Da, Mw 710000 Da, 27.5% added extender oil). The latter contains a highly aromatic oil, HAO, from the type DEA (distilled aromatic extract), with typical composition: 38% aromatic carbons, 26% naphtenic carbons, 36% paraffinic carbons (according to ASTM D2140), and viscosity value of 32 cSt (at 373 K). Rubber compounds were prepared in an open mill according to ASTM D3182 and subsequently vulcanized. More details on the sample preparation procedures are given in Ref. 4. Indeed, the HAO in SBR 1712 is the only material different from those included in SBR 1502 formulation, then SBR 1712 samples will be called hereafter composite samples.

Samples of vulcanized SBR 1502 and SBR 1712 were cut with a bistoury in a single pass in parallel direction to the rolling direction. Samples after the cut were examined with magnifying glass (X100) in order to check the sharpness of the resulting cut. Sample dimensions for DMA studies were around 40 mm length, 9 mm width and 2 mm thickness.

2.2. *Characterization methods*

DMA tests, loss tangent (damping or internal friction), $\tan(\phi)$ and dynamic shear modulus, G' were measured as a function of the applied electric field, E, in a mechanical spectrometer working in torsion at temperature of 300.0 K ($\pm$0.3 K), in air.

Damping was determined by measuring the relative half width of the squared resonance peak for a specimen driven into forced vibration using Eq. (1)[7]

$$\tan(\phi) = \frac{\omega_2 - \omega_1}{\omega_0}, \tag{1}$$

where ω_0 is the resonance frequency, and ω_1 and ω_2 are the frequencies at which the amplitude of oscillation has fallen to $1/\sqrt{2}$ of the maximum value. The errors of $\tan(\phi)$ and G', being proportional to the squared oscillating frequency, f, are less than 1%.

The relation between f and G' is given in Eq. (2),[7–10]

$$G' = \frac{(2\pi)^2 f^2 l \Pi}{k a^3 b}\, \alpha\, f^2, \tag{2}$$

where k is a constant which depends on the ratio b/a, II is the moment of inertia of the oscillating system, l is the length of the sample and a and b are the half-thickness and width of the sample, respectively.

The maximum oscillating strain on the surface of the sample was 1×10^{-4}. The electric field was produced by two electrodes placed at the sample position, lying in parallel direction to the torsion axis of the spectrometer, i.e., the resulting electric field is perpendicular to the torsion axis. Electrodes were connected to a variable DC high-voltage power supply, giving rise to E values up to 1000 kV/m at the sample location.

HAO (type DEA) oil viscosity measurements under electric field were performed in a vibration electromechanical viscometer in torsion. An atactic poly-methyl methacrylate (PMMA) parallelepiped reed oscillated in torsion along its larger axis in the space between two electrodes, which produced the electric field. Electrodes were connected to a variable DC high-voltage power supply from a Biddle megohmmeter, giving rise to E values up to 1000 kV/m. The reed and electrodes are immersed in the oil to be studied which was contained in a cubic cell constructed in PMMA with a volume of 350 cm^3. The oscillating reed was driven electromagnetically and the changes in viscosity were determined for measuring the square voltage (energy) to keep the oscillation at a given constant amplitude.[7] The oscillation angle for the reed was measured from a usual optical system based in a mirror and a photodiode and it was 1×10^{-3} radians. The oil bath was thermalized at 300.0 K ($\pm$ 0.3 K).

3. Theoretical Background

3.1. *Previous results*

3.1.1. *Magnetic memory effect in magnetite charged polypropylene composite*

The interaction mechanisms between magnetic particles embedded in a polymeric matrix was described by the model of Mocellini *et al.*[1] and it uses the following assumptions: (i) The magnetic particles are considered as magnetic dipoles. (ii) The particles (magnetic dipoles) are considered as spheres of radius, r, which are separated by a gap, d_0, Fig. 1. (iii) The position of the magnetic particles in the polymeric matrix is fixed and the only freedom of movement is a rotation. In fact, the particles can rotate around their dipole centers (geometric centers) for an alignment in the direction of the applied external magnetic field. (iv) Forces are acting on each dipole caused by elastic properties of the matrix, by magnetic fields of neighboring magnetic dipoles and by the external magnetic field. Consequently, it is either possible that a dipole returns to the original direction or it remains in a new direction when the external magnetic field is switched off. (v) One of the

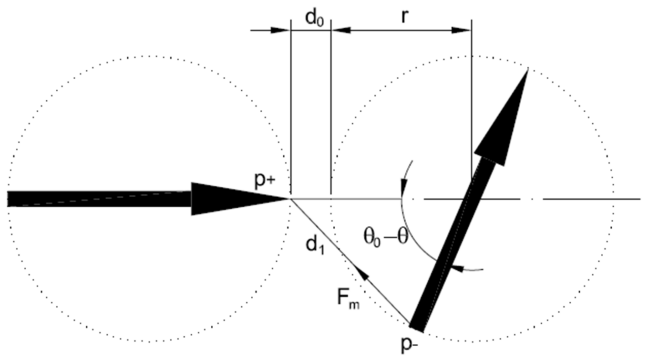

Fig. 1. Geometric representation of the magnetic moments for the equivalent dipole arrangement used in the mean field approximation considered in the work from Ref. 1.

dipoles is fixed in a given direction, and the other one is free to rotate for aligning.

Regarding the representation of magnetic dipoles shown in Fig. 1, it was demonstrated that considering the two particles having their centers on the same plane does not diminish the applicability of the model.[1]

In this model, three interacting magnetic and mechanical forces are considered where by two are intrinsic of the material and not dependent on the external magnetic field. The first magnetomechanical interaction is caused by the magnetic forces between two adjacent particles trying to align them, M_m. Secondly, as a consequence of the fixed positions of the centers of the particles, the deformation of the matrix during the rotation of the dipoles is taken into account. Thus, the second interaction is promoted by an elastic deformation of the matrix, M_G. As it can be inferred intuitively, the first and second contributions are counteracting. If the magnetic force tries to rotate a particle into a new position, the force caused by the elastic deformation of the matrix will work against the magnetic force. Finally, the third interaction is caused by the external magnetic field acting on the magnetic particle. The final direction of the particles is reached when all forces are in equilibrium.

The total intrinsic interaction was given by the algebraic sum of the magnetic interaction and the elastic contribution. In algebraic sum, counteracting forces lead to opposite signs of magnetic and elastic interaction. The positive sign for the magnetic moment when the rotation is clockwise was chosen. The calculated expression for the whole intrinsic magnetomechanical moment, M_T, is[1]

$$M_T = -11,6\pi r^3 Y\theta - G\frac{4\pi r^3}{\rho}\theta + \frac{C}{\sqrt{\rho+1}}\frac{\sin(\theta_0-\theta)}{\left[\frac{\rho^2/2+\rho+1}{\rho+1}-\cos(\theta_0-\theta)\right]^{3/2}} \quad (3)$$

where $\rho = d_0/r$ (see Fig. 1), $C = pg^2/(4\pi\mu_0 r\sqrt{2})$, p is the magnetic pole strength, μ_0 is the permeability of vacuum, θ_0 is the initial misorientation between two adjacent particles, θ is the rotation angle taken clockwise since θ_0 and Y and G are the Young's and shear modulus, respectively. The first and second terms in the right side of Eq. (3) correspond to the tensile and shear elastic response of the matrix, M_G, due to the rotation of the magnetic particles embedded in the polymeric matrix, respectively. The third term corresponds to the magnetic torsional moment, M_m, owing to the magnetic interaction between two magnetic particles, see for more details Ref. 1. The behavior of the moments mentioned above is a function of the torsion angle as shown in Fig. 2. Also shown in the figure is the behavior of the total intrinsic energy of the dipoles system as a function of the torsion angle, E_T, obtained from the integral relation with the moment, $E = \int M d\theta$. As it can be seen from Fig. 2, at the critical angle θ_{crit}, where the total intrinsic moment (M_T) is null, an unstable state of energy occurs, as expected. In the top of Fig. 2, particle orientations are schematically shown. At torsion angles higher than θ_{crit}, the particles will rotate as a consequence of the magnetic interaction going to a parallel state (indicated by point B in figure). This stage is represented by a minimum energy at which the particles have reached a new equilibrium position.

It is convenient to be mentioned here that, the ordinates in Fig. 2 are absent from numerical labels due to the fact that the moments and energy plotted in the Figure were calculated from arbitrary values of the parameters involved in the model. Indeed, the absolute value for moments and energy will change for different groups of parameter values to be chosen, but the whole trend of the curves and their relationship among them as a function of θ are the same.

The third interaction process is related to the interaction between the particles and an external magnetic field.

Then, the total magnetomechanical moment including an external magnetic field is obtained by adding the magnetic

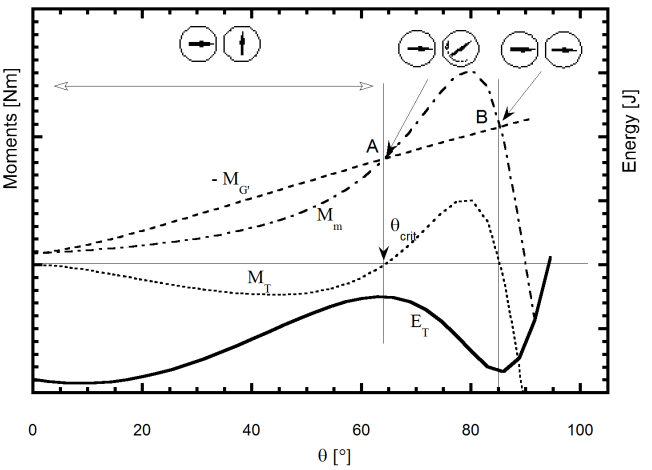

Fig. 2. Dependence of the magnetic and mechanical moments ($M_m, M_{G'}, M_T = M_m - M_{G'}$) and the energy ($E_T$) on the rotation angle θ. The curve of elastic moment M_G has been plotted multiplied by (-1). In the top of Fig. 2, dipole orientations at various angles θ are schematically shown; taken from Ref. 1.

Source: Ref. 1.

moment promoted by the external field to Eq. (3). As it can be inferred easily, the effect of the external magnetic field leads to a continuous movement of the dipole from its initial position up to the aligned state without passing through metastable positions.[1]

3.1.2. Electric inclusion

In this section, the concepts and equations related to the misfit of strain in composites or two-phase polymers for the case of dielectric materials will be introduced. The electric inclusion model takes the idea of partitioning the volume of the sample in small elementary cubes in such a way that each partitioned element is composed by a single phase, dipolar or nonpolar in the polymer material we are dealing with.[4] Figure 3 summarizes the main concepts for the case of dielectric materials. It shows a (z,y) plane of the partitioned sample at $x = v$, where the size of the partitioned matrix, over each axis, was chosen equal to lo_p. The model now starts with the following considerations:

(a) The volume element corresponding to a dipolar phase, located at (v, m, j) of the whole partitioned matrix, which is plotted by means of full fine lines in Fig. 3, is cut and removed out of the matrix, leading to a cubic hole of edge lo_p.
(b) An electric field is applied to this extracted dipolar zone, then it stretches from lo_p to $lo_p + \in lo_p$, with $0 \leq \in \leq 1$, see broken lines in Fig. 3. It is easy to recognize that the mismatch parameter $\in$ is the strain misfit promoted thorough an electrostrictive phenomenon.[11,12] Indeed, the application of the electric field gives rise to the appearance of an inclusion of larger size into the matrix, plotted by means of broken lines.
(c) The inclusion of size $lo_p + \in lo_p$, with $0 \leq \in \leq 1$, plotted by means of broken lines, will be firstly compressed to fit into the hole of the matrix and subsequently placed in.
(d) The inclusion is mechanically released and then the boundaries of the hole, in the z-axis, displaced to a position $lo_p + \beta \in lo_p$, with $0 \leq \beta \leq 1$, where the equilibrium of stresses is achieved. The wide lines in Fig. 3 represent this state.

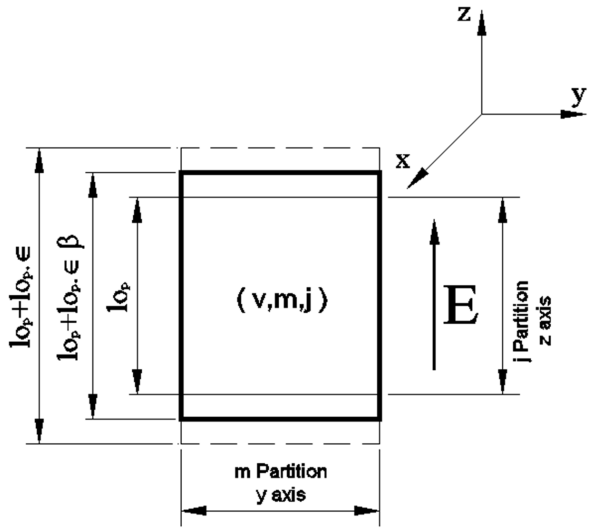

Fig. 3. Equilibrium position of the boundary between the dipolar inclusion and the matrix, after location of the stretched inclusion into the matrix hole and release of its constriction. See explanation in the text.

Therefore, by means of the above-described procedure, the elastic misfit promoted by an electric dipole when an electric field is applied, can be studied using the mathematical formalism of the inclusions theory. In fact, β is the misfit coefficient, which is related to the matrix strain caused by the stretching of the dipole when the electric field appears, and it takes the form[4–6]

$$\beta^z = \frac{1}{1 + \left(\frac{M_m}{M_i}\right) \cdot \left(\frac{fr_i^z}{fr_m^z}\right)}, \tag{4}$$

where M is the Young modulus, fr is the volume fraction and the sub-indexes m and i correspond to the matrix free of electrostrictive effects and to the inclusion (stretched dipole) elements, respectively. The volume fractions satisfy $fr_i + fr_m = 1$. The supra-index "z" indicates that the direction for the study of the problem is the z axis. By working mathematically, it was shown that β coefficient can be calculated, despite not knowing the elastic modulus of the dipolar zone (M_i), from[4]

$$\beta = fr_m \frac{M}{M_m}, \tag{5}$$

where M refers to the Young's modulus of the whole material when electrostrictive effects appear, i.e., the material containing the matrix and the dipolar inclusions is stressed. Indeed, Eq. (5) makes it possible to calculate the misfit coefficient in dielectric materials, or two-phase polymers, knowing the elastic modulus of the matrix, free of electrostrictive effects, its volume fraction and the elastic modulus of the whole material, when the electrostrictive effects appear.[4,13,14] Besides, the mechanical energy transfer related to the electrostriction phenomenon is due to the movement of the borders of the inclusion into the matrix from its initial compressed state up to the achievement of the mechanical equilibrium condition.[4] The expression for the ratio between the elastic energy transferred to the matrix, W_m^z and the whole available one, W_T^z (over the z-axis)[13,14] takes the form,[4]

$$\frac{W_m^z}{W_T^z} = \frac{M_m - M\, fr_m}{M} \beta^2 \frac{1}{fr_m}. \tag{6}$$

The ratio given by Eq. (6) is very intuitive regarding the competition of the moduli values between the inclusion and the matrix, until the equilibrium condition is achieved.

3.2. *The new model*

Considering the thermodynamic correlation between the dielectric polarization and electric field vectors on the one hand and magnetization (or magnetic polarization) and magnetic field on the other hand, the results from the magnetic case shown in Sec. 3.1.1 can be straightforwardly applied to electric materials.[11,12] Therefore, it could be possible that in a dielectric liquid, the retention of electrical dipoles in an aligned direction occurs due to the intrinsic interaction between them.

Moreover, the equations for the magnetic case during the dipolar orientation process can be straightforwardly extrapolated to the electrical case due to the parallelism between the magnetic and electric mathematical structures.[1] Nevertheless, the counteracting term from the elastic contribution from the matrix must be replaced for an appropriate representation of a viscous fluid without the elastic restoration behavior.[15]

In the present work, our model describes the interaction mechanisms between polar molecules in HAO type DEA oil in SBR 1712 samples after the alignment between them has occurred.

Straightforwardly to the model summarized in Sec. 3.1.1,[1] it uses the following assumptions:

(i) Electrical dipoles will be considered as spheres of average radius, r, with a superficial charge density, λ_d, separated by a gap d_0 between them, Fig. 4(a). In order to handle the mathematical expressions easily from the point of view of applications in engineering, the dipolar molecule will be considered as a single resulting dipole which concentrates on the superficial charge density in two punctual charges, q, located in opposite points over the diameter of a sphere, which lies in the direction of the real molecular dipolar axis, Fig. 4(b). This representation will be called hereafter the average dipole configuration. Therefore, from a view in a plane, a geometrical representation similar to the considered one for the magnetic case can be adopted, as shown in Fig. 5. The mean field approximation for the concentration of the superficial density of charge in two punctual ones only implies a mismatch between both representations of $2/\pi$ (see Appendix A), so, it does not obstruct the subsequent analysis made in the present work.

(ii) The polar molecules are considered to be randomly distributed in the viscous liquid.

(iii) The position of the average dipoles in the viscous liquid is fixed and the only freedom of movement is a rotation. In fact, the average dipoles can rotate around their dipole centers (geometric centers) for an alignment in the direction of the applied external electric field. This assumption, even if it is restrictive for the movement of dipoles in a viscous liquid, has the sole object of simplifying the mathematical study of the rotational behavior and it does not diminish the obtained results.

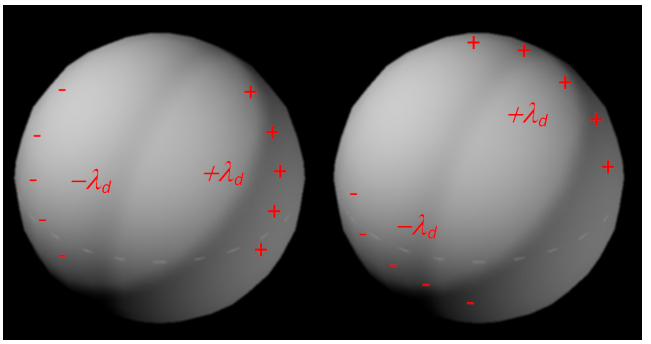

(a)

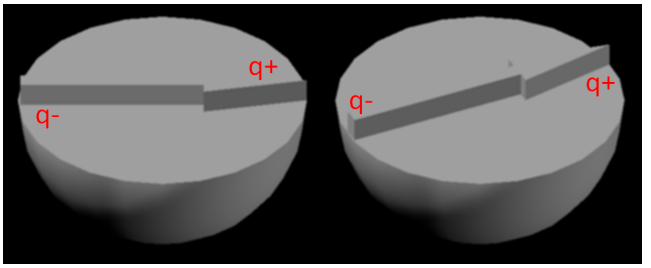

(b)

Fig. 4. (a) Spherical dipolar molecules in the dielectric liquid, exhibiting a superficial density of charge λ_d. (b) Average dipole configuration obtained by concentrating the two charges punctually on opposite positions over the diameter of the dipolar sphere. See explanation in the text.

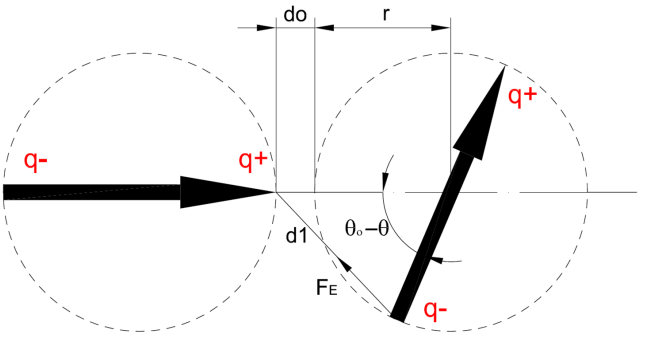

Fig. 5. Two-dimensional view of the average dipole configuration.

Indeed, the resulting expressions also allow considering the effect from the movement of dipoles along a line undergoing the dipolar centers.

As it can be inferred from Fig. 5, by applying an external electric field, the average dipoles will rotate around their dipole centers until an alignment in the direction of the applied external electric field is achieved. In addition, let us assume that once the alignment has been achieved, the average dipoles are retained in an aligned manner between them after the electric field is switched off.

The expression for the intrinsic electric moment for keeping the alignment between the two average dipoles,

M_E, has the form of the last term in Eq. (3), thus

$$M_E = \frac{C}{\sqrt{\rho+1}} \frac{\sin(\theta_o - \theta)}{\left[\frac{\rho^2}{2}+\rho+1}{\rho+1} - \cos(\theta_o - \theta)\right]^{3/2}}, \quad (7)$$

where ρ, θ and θ_0 have the same meaning as in Eq. (3), see Fig. 5, and C for the present electric case equals $q^2/(2r\pi^2\varepsilon\sqrt{2})$, with ε the permittivity of medium. This value is similar to C constant for the magnetic case, but for the electric case it is divided by the factor $2/\pi$, which comes from the charge concentration procedure from λ_d in the average dipole representation.

Moreover, as our present study is performed once the alignment state was achieved, so, $\theta_0 = 0$ (see Fig. 5) and then Eq. (7) can be rewritten as

$$M_E = -\frac{C}{\sqrt{\rho+1}} \frac{\sin(\theta)}{\left[\frac{\rho^2}{2}+\rho+1}{\rho+1} - \cos(\theta)\right]^{3/2}}. \quad (8)$$

The electrostatic interaction given from M_E has the capability of being a counteracting effect for keeping aligned the dipoles in the liquid against some external perturbations as for instance, mechanical stress or increase in temperature, etc., which lead to an increase in the dipolar vibration. The aligned dipoles can rotate or oscillate clockwise or counter-clockwise around the alignment direction in such a way that the electrostatic interaction plays a role alike the counteracting elastic effect, then, this behavior will be called hereafter electroelasticity. Indeed, the behavior of M_E (Eq. (8)) as a function of the rotation angle, Fig. 6, shows a positive or negative counteracting response depending on the direction of dipole rotation promoted by an external perturbation, clockwise or counter-clockwise, respectively; in agreement with the above exposed. As it can also be seen from the figure, the capability for restoring the dipoles to the aligned position decreases as $\rho = d_0/r$ increases due to the decrease in the electric interaction as the gap between molecules increases as expected.

The HAO type DEA oil has no counteracting contribution in order to keep either aligned or misaligned dipoles because the elastic modulus is null in a viscous liquid.[15] However, the viscosity of liquid modifies the dynamic response of the system.[16,17]

By using the general equation for the relation between energy and the electric moment, M_E, with respect to the rotation angle $\theta(E = -\int M\, d\theta)$, the energy, E_E, takes the form

$$E_E = \frac{C}{\sqrt{\rho+1}} \int \frac{\sin(\theta)\, d\theta}{\sqrt{[a - \cos(\theta)]^3}}, \quad (9)$$

where $a = (\rho/2 + \rho + 1)/(\rho + 1)$. Integrating Eq. (9) we have

$$E_E = -\frac{C}{\sqrt{\rho+1}} \frac{2}{\sqrt{a - \cos(\theta)}} + A, \quad (10)$$

wherein A is the integration constant. On assuming that for the angular position where the moment is null, the energy equals zero, A can be calculated thus

$$A = \frac{2C}{\sqrt{(\rho+1)(a-1)}}. \quad (11)$$

Therefore, Eq. (10) can be rewritten as

$$E_E = -\frac{2C}{\sqrt{\rho+1}} \left\{ \frac{1}{\sqrt{a - \cos(\theta)}} - \frac{1}{\sqrt{a-1}} \right\}. \quad (12)$$

The behavior of E_E as a function of the torsion angle around the equilibrium angular position, in the aligned state, for different ρ values is shown in Fig. 7. It can be seen from the figure that the minimum energy occurs for the aligned position and that the whole values of E_E decreases as

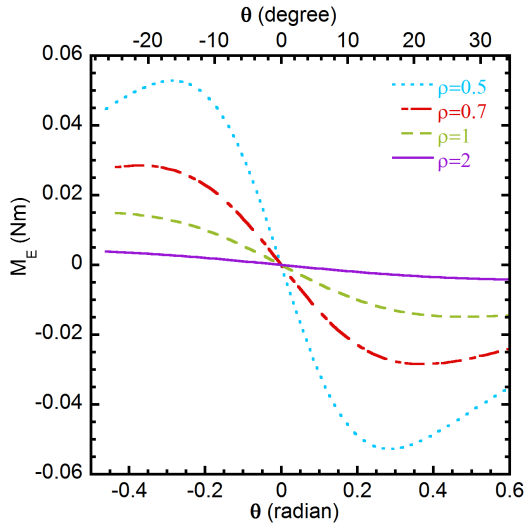

Fig. 6. Electrical moment, M_E as a function of the rotation angle, θ, (Eq. (8)) for different values of $\rho = d_0/r$.

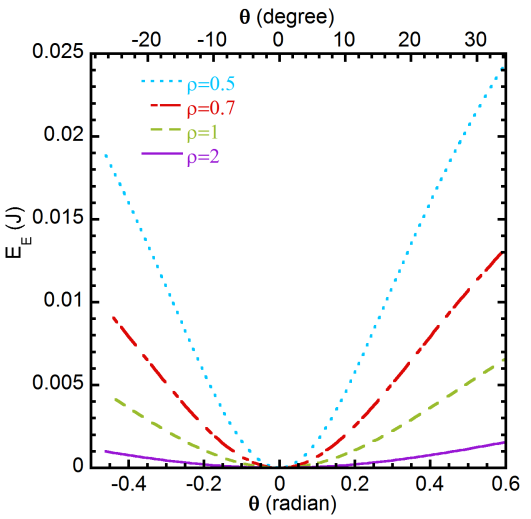

Fig. 7. Energy, E_E as a function of the rotation angle, θ, (Eq. (12)) for different values of $\rho = d_0/r$.

ρ increases, in agreement with the behavior shown by M_E in Fig. 6.

Besides this, the electrostatic force, F_E, between two neighbor average dipoles lying in the aligned state can be written from the usual form[11,12]

$$F_E = \frac{1}{4\pi\varepsilon}\frac{q^2}{d_1^2}. \tag{13}$$

In order to obtain the electrostatic force as a function of θ, the cosine theorem is applied in relation to d_1 such that (see Fig. 5)

$$d_1^2 = (d_o + r)^2 + r^2 - 2(d_o + r)r\cos(\theta_o - \theta). \tag{14}$$

By working mathematically, Eq. (14) can be written as

$$d_1^2 = r^2[(\rho+1)^2 + 1 - 2(\rho+1)\cos(\theta_o - \theta)]. \tag{15}$$

Then, the electrostatic force as a function of θ results,

$$F_E = \frac{1}{2\varepsilon}\frac{q^2}{2\pi r^2} \times \frac{1}{[(\rho+1)^2 + 1 - 2(\rho+1)\cos(\theta_o - \theta)]}. \tag{16}$$

The behavior of F_E as a function of the torsion angle around the equilibrium angular position in the aligned state, for different values of ρ, is shown in Fig. 8. The maximum electrostatic force is achieved for the aligned state, as it could be assumed intuitively.

It can also be inferred from Eq. (16) that dipoles are subjected to a state of compression mechanical stresses among them, as shown by means of fine arrows in Fig. 9. The compressive stresses among aligned dipoles decrease the capability of movement of the dipoles in the liquid giving rise to an increase in its viscosity, as discussed in the following paragraphs. In addition, compressive internal stresses also take place inside each dipole.

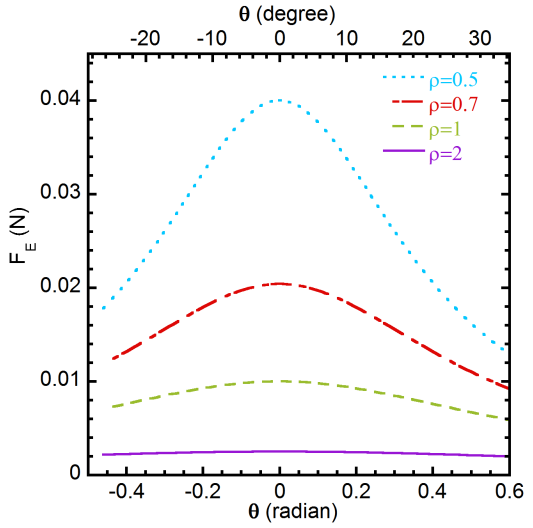

Fig. 8. Electric force, F_E, as a function of the rotation angle, θ, (Eq. (16)) for different values of $\rho = d_0/r$.

A proportional value to an effective modulus related to the electroelastic behavior, for the aligned state after the suppression of the electric field, can be calculated from the derivative of M_E, Eq. (8), with respect to the rotation angle, that is,

$$\frac{\partial M_E}{\partial\theta} = \frac{C}{\sqrt{\rho+1}}\left\{\frac{\cos(\theta)}{\left[\frac{\rho^2/2+\rho+1}{\rho+1} - \cos(\theta)\right]^{3/2}} - \frac{3}{2}\frac{(\sin(\theta))^2}{\left[\frac{\rho^2/2+\rho+1}{\rho+1} - \cos(\theta)\right]^{5/2}}\right\}. \tag{17}$$

Evaluating Eq. (17) at $\theta = 0$, we have

$$\left.\frac{\partial M_E}{\partial\theta}\right|_{\theta=0} = \frac{C}{\sqrt{\rho+1}}\left\{\frac{1}{\left[\frac{\rho^2}{2(\rho+1)}\right]^{3/2}}\right\}. \tag{18}$$

Considering that $r = d_0/\rho$ and replacing the value for the C constant in Eq. (18), it results in

$$\frac{\partial M_E}{\partial\theta} = \frac{q^2(\rho+1)}{2d_o\pi\varepsilon\rho^2}. \tag{19}$$

In fact, we have obtained the value of an effective electroelastic modulus around the aligned angular position from the slope of M_E at around $\theta = 0$, as it is usual in the theory of the crystalline solids.[18,19] However, this value of effective electroelastic modulus comes from the electrostatic interaction of electric dipoles, which is in contrast to the attractive and repulsive contributions from the potentials theory in crystalline solids through Condon–Morse curves.[18,19] Moreover, this effective modulus has a local effect in the region close to the dipoles, so, it cannot be extrapolated to the whole fluid due to the nature of the liquid.[15]

The electric dipoles in a highly aromatic mineral oil are mainly located in the zone of the bonding between

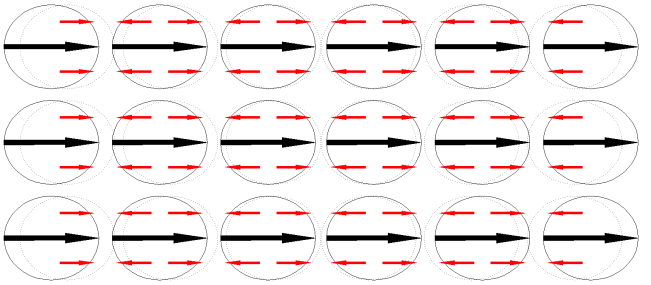

Fig. 9. Internal stresses state of the dipoles which remain in aligned state after the electric field is switched off. Compressions stresses occur inside each dipole and also between neighbor dipoles which leads to a whole compressive effect of the liquid. Circles in full lines: Dipoles prior to suffering the compression stresses. Circles in broken lines: Dipoles suffering the compression stresses.

the hydrocarbonated chains and the aromatic rings.[20,21] By rotating the polar groups in a dielectric oil due to the application of an external electrical field, the hydrocarbonated chains will suffer stretching or compressing giving rise to an increase in their free energy. It decreases the mobility among the chains which is equivalent to an increase in the viscosity of the whole liquid. In addition, the compression stresses among dipoles, located at different chains, promote an increase in the coordination and connection between chains leading also to an increase in the viscosity. Consequently, we could assume that locally around two neighborhood dipoles, the electroelastic effective modulus can be represented from a parallel with the theory of elasticity of the continuous media through an apparent shear modulus G_{app}, that is (see Fig. 10);

$$G_{app} = \frac{\tau}{\tan(\gamma)}, \tag{20}$$

where τ was considered as the ratio between the mechanical applied force, F, and the half of the sphere surface for the dipoles. F and/or τ are external perturbations which attempt to misaligning the dipoles. For small θ angles and working mathematically, we can write

$$F = G_{app}\frac{2\pi r^3}{d_o}\theta. \tag{21}$$

The equation for the mechanical moment, M_{mech}, can be easily obtained by replacing the value for the force from Eq. (21) in the expression $M_{mech} = rF$, then M_{mech} results

$$M_{mech} = G_{app}\frac{2\pi r^3}{\rho}\theta. \tag{22}$$

Taking the derivative of Eq. (22) with respect to the torsion angle, we obtain

$$\frac{\partial M_{mech}}{\partial \theta} = G_{app}\frac{2\pi r^3}{\rho}. \tag{23}$$

By relating Eq. (19) with (23), we obtain a local mechanical constrain around the neighbor zone to the dipoles, through an apparent shear modulus promoted by the electroelasticity, which equals

$$G_{app} = \frac{q^2(\rho+1)}{2d_o\pi\varepsilon\rho^2}\frac{\rho}{2\pi r^3}. \tag{24}$$

Remembering that the dipolar moment, μ, takes the form $\mu = 2rq$,[11,12] Eq. (24) can be written as

$$G_{app} = \frac{\mu^2}{16\pi^2 r^6\varepsilon}\frac{(\rho+1)}{\rho^2}. \tag{25}$$

From Eqs. (24) and (25), it can be observed that the electroelastic strength increases both as the amount of charges in the dipoles increases and when the gap between them decreases, as it could be expected. Therefore, an increase in the strength of the apparent modulus leads to an increase in the capability of linking between the dipoles lying on the carbon chains (after they achieved the aligned state). It promotes a decrease in the mobility of hydrocarbonated chains giving rise to an increase in the whole viscosity of the HAO type DEA oil. In fact, from a viscosity test as described in Sec. 2.2, the rotating reed records the changes in the viscosity of the fluid by measuring the change in the mobility of the hydrocarbonated chains as a function of the applied electric field.

The theoretical results obtained here about the change in the viscosity in HAO type DEA oil, promoted by the electric field, are applied in the next section to viscoelastic inclusions of the same oil embedded in a SBR matrix for explaining electric memory effects in SBR 1712 samples.

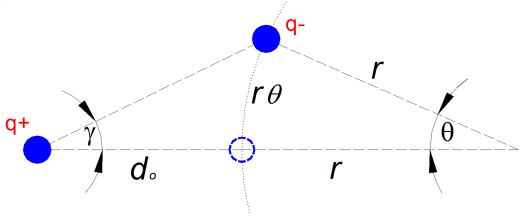

Fig. 10. Electroelastic parallel: The negative charge for the dipole at the right side from the figure moves from the aligned position (circle in broken lines) toward a misaligned state (full circle). See explanation in the text.

4. Results and Discussion

Figure 11 shows the behavior of both the dynamic shear modulus, G', for a composite SBR 1712 sample (full circles) and the relative viscosity for HAO (type DEA) oil (full triangles), as a function of the applied electric field strength; measured during the increase in field. As it can be seen from the figure, the dynamic modulus increases as the strength in the electric field increases, because the electric field promotes the stretching of dipoles (polar groups) along the direction of the electric field; giving rise to the appearance of inclusions (see Sec. 3.1.2).[2–4] In fact, as the electric field increases, higher modulus values in the inclusion are promoted due to the increase in the stretching of the dipoles until saturation. The orientation phenomenon from the dipoles could contribute also to the increase in the modulus. Indeed, an increase in the electric field promotes stronger pinning of the oriented dipoles along the field direction, so the larger anchorage of the dipoles leads to higher torsion modulus of the inclusions, as the field increases.[4] Consequently, the increase in the modulus of the inclusions, both by stretching and/or rotation, leads to an increase in the modulus of the whole matrix; as it is well known in the mechanical properties of composite and two-phase materials.[2,3,22]

It is convenient to mention here that the viscosity of the HAO (type DEA) oil is high enough at both the frequency

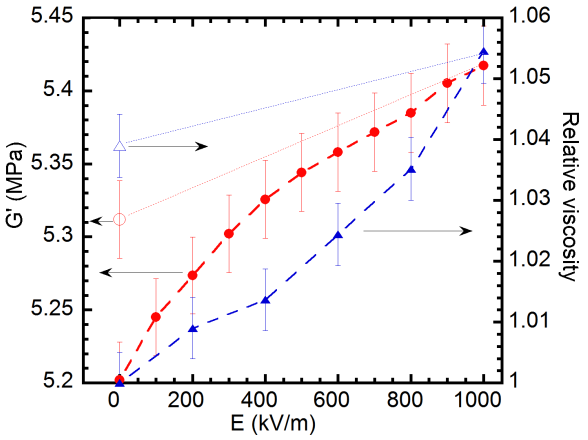

Fig. 11. Dynamic shear modulus, G', (left axis, circles) and relative viscosity = viscosity as a function of electric field divided by the initial value of viscosity at null field (right axis, triangles), as a function of the external electric field, E. Full symbols: Measured values during the electric field increase. Empty symbols: Measured values at $E = 0$ after having reached the maximum field value. Lines are a guide for the eyes.

(≈ 2 Hz) and temperature 300.0 K (± 0.3 K) used in the present work, in such a way that this phase in the SBR 1712 composite samples can be considered as a viscoelastic solid.[4,16]

The behavior of $\tan(\phi)$ curves as a function of the applied electric field for SBR 1712 composite samples follows the usual trend earlier reported for DMA experiments conducted under high electrical field.[4–6] Thus, the higher the increase of modulus values as the field strength increases, the higher the decrease of $\tan(\phi)$ values. This behavior of $\tan(\phi)$ is in agreement with the above mentioned regarding the development of internal stresses in the polymer matrix promoted by the electric field. The increase in internal stresses in the polymer matrix acts like obstacles which difficult the movement of its chains leading both to the decrease in the damping values and to the increase in the modulus values.[1,4–6,17,23,24]

The viscosity of HAO (type DEA) oil increases as the strength in the field increases due to the stretching, rotation and rearrangement of dipoles located in the oil. As said before, the electric dipoles in a highly aromatic mineral oil are mainly located in the zone of the bonding between the hydrocarbonated chains and the aromatic rings.[20,21] The stretching of dipoles promotes an increase in the internal stresses in the region of oil between the electrodes and then the mobility of the hydrocarbonated chains decreases leading to the increase in the viscosity of the oil in such zone. In addition, the rotational and rearrangement effects of dipoles controlled by the electric field are another two overlapped effects contributing to an increase in the viscosity of the liquid. In fact, the rotation of dipoles promotes stretching or compression stresses along the hydrocarbonated chains leading to the decrease in their capability of movement, giving rise to an increase in the viscosity. Moreover, dipoles can be moved by the field in order to increase the mutual overall interaction among them in the oil by decreasing their gap, giving rise to higher degree of correlation among chains, leading to an increase in the viscosity.

On the other hand, the DMA response for SBR 1502 does not exhibit change in both G' and $\tan(\phi)$ as a function of the field strength. So, the electrostrictive effects in SBR 1712 are promoted by the HAO (type DEA) oil in agreement with previous work.[4]

It should be highlighted that after reaching the maximum electric field value (1000 kV/m) and subsequently remeasuring at null field both the modulus in the composite SBR 1712 sample and the viscosity in the HAO (type DEA) oil, a behavior of memory was found out. In fact, the modulus and viscosity are different from zero exhibiting a hysteretic effect; see empty symbols in Fig. 11. In addition, the $\tan(\phi)$ values also exhibit memory behavior, retaining smaller values than the starting one, prior to the beginning of the field increase (results not shown in Fig. 11); in agreement with the above mentioned. In contrast, for maximum electric field values up to 420 kV/m, a memory behavior in both the damping and the modulus was not found, i.e., measured values during the decrease in the field intensity are in good agreement with those measured during the field increase. It is in agreement with previous results obtained in SBR 1712 samples up to field strengths of 420 kV/m.[4] Besides this, for HAO (type DEA) oil, the appearance of a memory behavior once returned to null field after having reached 420 kV/m could not be assured due to both the small change in viscosity at this field strength and the error bandwidths.

The memory behavior found in both G' and $\tan(\phi)$ in composite SBR 1712 samples after subjecting the samples at the highest electric field, points out that the increase in the internal stresses in the inclusions promoted by the electric field is the result of overlapping the effects of stretching and rotation of dipoles. In fact, after switching off the electric field, the stretch behavior on the dipoles disappears but the remainder orientation process between dipoles can take place. Moreover, it is in agreement with both the memory behavior found for the viscosity of HAO type DEA oil shown in Fig. 11 and with the model developed in Sec. 3.2. The rotation of dipoles lying mainly in the zone of the bonding between the hydrocarbonated chains and the aromatic rings, for mineral oils, promotes stretching or compression stresses along the chains leading to the decrease in their capability of movement. It gives rise to an increase either in the viscosity, for the liquid,[15] and in the modulus, for the viscoelastic inclusion.[2,3,16,17,23,24]

In order to explore the behavior of the internal stresses during the field increase and after it is switched off, the behavior of β coefficient and the ratio W_m^z/W_T^z, as a function of the applied electric field, calculated by means of Eqs. (5) and (6), respectively are shown in Fig. 12. Plotted values start from the first stage in the electric field, due to the electric

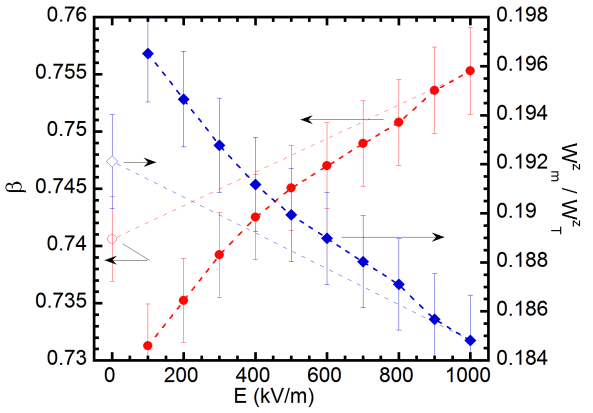

Fig. 12. Misfit coefficient β (left axis) and W_m^z/W_T^z (right axis) as a function of the electric field strength calculated for SBR1712 composite samples. Lines joining the points are a guide for the eyes. Full symbols: Measured values during the field increases. Empty symbols: Measured values at $E = 0$ after having reached the maximum field value.

inclusion model and can be applied after the appearance of the inclusion promoted by the electric field application, see Fig. 3 in Sec. 3.1.2. It has to be mentioned that in all the calculations made in the present work, the dynamic elastic shear modulus, G', instead of the Young modulus, has been used. Nevertheless, it does not diminish nor obstruct the subsequent analysis made here, since the material under study is considered through a mean field approximation.[1,4,13,14] As it can be seen from Fig. 12, as the electric field increases, β increases and W_m^z/W_T^z decreases. The increase in β values indicates that the increase in the strain misfit is mainly accommodated by the matrix, i.e., $\beta \to 1$ leads to $lo_p + lo_p \in \beta \to lo_p + lo_p \in$ (see Fig. 3). The electric field increase promotes an increase in the modulus of the inclusion forcing the matrix to accommodate higher strain misfit, leading to an increase of β.[4] Besides, an increase in the modulus of the inclusion with respect to the modulus of the matrix leads to a decrease in W_m^z/W_T^z, see Fig. 12. It indicates that the work done in compressing the inclusions from $lo_p + lo_p \in$ up to lo_p for being introduced into the matrix holes, see Fig. 3 in Sec. 3.1.2, as the electric field increases, is larger than the work done by the matrix. A larger work is required for compressing the inclusion in a magnitude $\in$ as the electric field increases due to the increase in the modulus of the inclusion promoted by the increase in the electric field.

It should be pointed out that despite the error bandwidths, the β coefficient and the ratio W_m^z/W_T^z exhibit a change in slope at around 420 kV/m. Moreover, the values for both β and W_m^z/W_T^z at 420 kV/m are near the values measured after the field was switched off (see empty symbols in Fig. 12). Therefore, we could assume that above 420 kV/m the driving force controlling the electrostriction mechanism has changed. Below 420 kV/m, both stretching and rotation of dipoles take place, in contrast, above 420 kV/m, the rotation of dipoles lying in the hydrocarbonated chains could be the predominant driving force. This assumption could be in reasonable agreement with the fact that larger stresses should be invoked by the dipoles for stretching or compressing the hydrocarbonated chains in the viscoelastic oil. Consequently, the physical mechanism leading to the increase in the modulus of the inclusion, which controls the behaviors in β and W_m^z/W_T^z, is not a misfit problem, as the one shown in Fig. 3 as it is related to a modification in the internal stresses in the inclusions for the stretching or compressing of the hydrocarbonated chains. Therefore, the usual relation between the strain and the square of the electric field strength in a dielectric material, related to the electrostrictive phenomenon goes fall.[11,12] In fact, the mechanical configuration of dipole rotation stretching or compressing the chains can be easily considered as an electric torque working over a spring. Then, the increase in internal stresses into the inclusion will exhibit a linear dependence on the applied field, which results in agreement with the behaviour of β and W_m^z/W_T^z over 420 kV/m in Fig. 12.

As discussed above, the appearance of memory behavior in the DMA response (modulus and damping), Fig. 11, and in the internal stresses, Fig. 12, is related to the rotational effects of dipoles through a retention process, as the one developed in the model from Sec. 3.2. Indeed, the value of G' for the composite sample after the field switch-off can be related to the value of the electroelastic modulus obtained for the memory model for dielectric liquids, Eq. (7). By considering that the applied external stress is transmitted uniformly through the composite sample, i.e., the Reuss condition,[2] the well-known relationship between the elastic modulus of the composite, G', and the moduli of the inclusion, G_i' and the matrix, G_m', can be written as

$$G_i' = \frac{fr_i}{\frac{1}{G'} - \frac{fr_m}{G_m'}}. \tag{26}$$

As G_i' is the elastic modulus for the inclusion exhibiting retained dipoles, then we can relate it with Eqs. (25) and (26), thus

$$G_i' = \frac{fr_i}{\frac{1}{G'} - \frac{(1-fr_i)}{G_m'}} \approx G_{\text{app}} = \frac{\mu^2}{16\pi^2 r^6 \varepsilon} \frac{(\rho+1)}{\rho^2}. \tag{27}$$

The theoretical model developed in Sec. 3.2 was performed for a liquid medium, so the sole driving force acting for the appearance of the memory, i.e., to keep the alignment between dipoles, is the electrostatic interaction between them or the so-called electroelastic effect. However, in the present study, the oil inclusion is considered as a viscoelastic solid due to the frequency and temperature used in the DMA tests. Thus, a counteracting effect from the viscoelastic contribution during the aligning process overlapped with the electric moment contribution could occur.[1] As it can be easily assumed, this counteracting effect diminishes the capability of aligning dipoles by the electric field, as shown in Ref. 1.

As it can be inferred from Eq. (27), the modulus of the inclusion G_i' is related to the electroelastic modulus, so, the electrostriction effect is entirely related to the HAO. Therefore, the permittivity (ε) in Eq. (27) corresponds to the HAO medium and it is not related to the composite.

For electrical tests performed on the composite involving direct current excitations, the whole permittivity could be a pondered addition of the permittivities corresponding to the matrix and the inclusion. In addition, electrical experiments performed in the frequency domain could lead to different relaxation processes appearing at different frequencies for each component of the composite, as it was shown in previous work related to the dielectric relaxation in two phase materials.[25]

Moreover, as it can be inferred intuitively, a viscoelastic behavior from the inclusions of HAO (type DEA) oil in the SBR matrix is in good agreement with the mechanical representation for the rotation of dipoles which stretch or compress the hydrocarbonated chains in the oil, as mentioned above.

After the field is suppressed, the viscoelastic contribution could play against the electroelastic contribution for keeping the electric dipoles aligned, if the minimum energy configuration is achieved only for the internal stress state prior to the application of the electric field.[1] It was shown in Sec. 3.1.1 that a metastable minimum energy state could occur even during the application of the field, which allows to retain the aligned state for the dipoles, when a counteracting elastic effect appears.[1] Then, if not all the dipoles are retained due to the electroelastic interaction, the volume fraction of electric inclusions will be smaller than the initial value considered in the electric inclusion model (Sec. 3.1.2). For a given value of elastic modulus of composite SBR 1712 sample exhibiting memory, G', the decrease in the volume fraction of inclusions (fr_i) leads to an increase in the values of the elastic modulus of the inclusions exhibiting memory, G_i', Eq. (26), Fig. 13. Therefore, the calculated value for G_i' obtained with the whole value of fr_i (27.5%, see Sec. 2.1), i.e., all the volume fraction of inclusions exhibits memory effects, is of maximum value.

Despite the three unknown incognita in Eq. (27), $\mu = 2rq$, r and d_0, from considering both an estimation of the dipolar size from the shape of the chemical molecule and the dipolar moment value reported for similar molecules, Eq. (27) can be used for obtaining an approximate solution of the gap among the dipolar moment arrangement in the dielectric inclusion. The procedure is as follows: (i) Figure 14 shows the behavior of G_{app} (Eq. (27)) as a function of $\rho = d_0/r$, for different values of dipolar moment, μ, and for a dipolar radius of 4 Å. This radius could be reasonable for large macromolecules like those involved in HAO (type DEA) oil.[20,21] (ii) By taking into consideration that the memory value of G' for the composite sample after the suppression of the electric field (see empty circle in Fig. 11) is related to the G_{app} through Eq. (27), (iii) By calculating the value of G_i' from Eq. (26) corresponding to the memory value measured for G'. (iv) By choosing a typical value for μ for dielectric compounds with aromatic rings (around 1.23×10^{-10} C m (0.37 D)).[20,21] (v) Interpolating a curve for the chosen μ value among the whole set of G_{app} versus ρ curves for different μ values, see the full line in Fig. 14, (vi) By taking the intersection of a horizontal straight line at the value of G_i' with the interpolated curve for the electrical moment, see arrows in Fig. 14. Finally, a value for ρ can be obtained. As said before, by considering a possible change in the volume fraction in the inclusion for the memory effect, the calculated value of ρ represents a maximum value. So, the smaller the volume fraction, the smaller the ρ value.

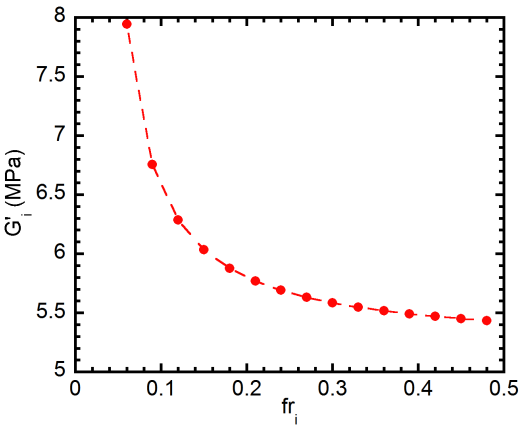

Fig. 13. Dynamic shear modulus for the inclusion as a function of the inclusion volume fraction, calculated from Eq. (26).

The calculated value for G' in the present study from Eq. (26) was 5.6 MPa. As it can be deduced from Fig. 14, for a given μ, the larger ρ is, smaller is the dipolar radius, r.

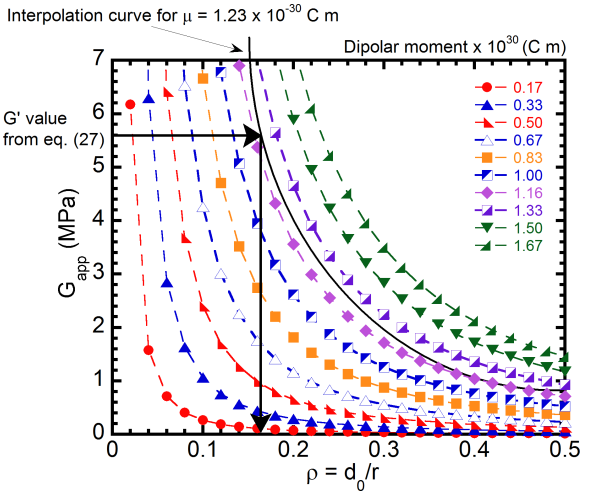

Fig. 14. Electroelastic modulus or apparent shear modulus calculated from Eq. (27) as a function of the parameter ρ, for a dipolar radius of 4×10^{-10}m, for different values of dipolar moment, μ. Full line: interpolated curve for $\mu = 1.23 \times 10^{-10}$ C m (0.37 D). Arrows see explanation in the text.

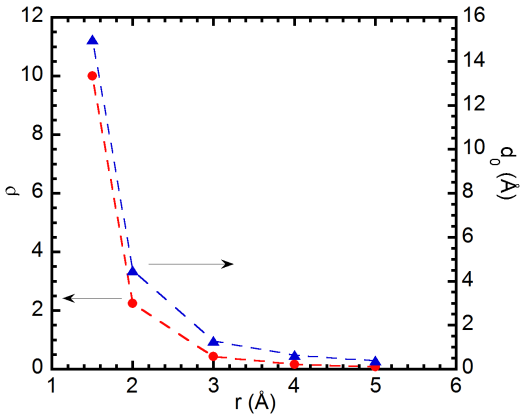

Fig. 15. $\rho = d_0/r$ (left axis) and d_0 (right axis) as a function of the dipolar radius.

Figure 15 shows the behavior of ρ as a function of the radius, r (left axis) for $G_{app} = 5.6$ MPa, determined from a set of G_{app} versus ρ curves for different radii, r, following the procedure described in Fig. 14. As a consequence of the definition of $\rho = d_0/r$, the value of the gap between dipoles, d_0, can be easily obtained. It is interesting to note that for radius value larger than 3, the gap between dipoles is smaller than the dipolar radius. Moreover, the behaviours of ρ and d_0, for values of r larger than 3, go to an asymptotic trend. Therefore, we could infer that the maximum gap between dipoles in HAO (type DEA) oil inclusions could be around 0.5 Å.

It should be highlighted that the procedure described here could be a useful tool for obtaining information about the spatial arrangement of dipoles in different formulations of dielectric composites or two-phase materials.

5. Conclusions

DMA studies performed under electric field have shown that SBR 1712 composite samples, which contain highly aromatic oil, exhibit memory effects giving rise to dynamic elastic modulus, damping and internal stresses degree which can be tailored depending on the applied electric field strength. In fact, after applying an electric field of 1000 kV/m, higher elastic modulus, higher internal stresses and lower damping values, than the ones prior the increase in the field strength, are achieved. The driving force controlling this mechanical response is the memory behavior which has taken place in the viscoelastic oil inclusions. The memory effects are controlled by the stresses from the stretching or compressing of the hydrocarbonated chains promoted by the dipole rotation up to the achievement of the aligned state and its subsequent retained condition.

The model for describing the memory effect in dielectric composite materials, due to the dipolar interaction of retained aligned neighbor dipoles, located at the inclusions, was successfully applied.

Moreover, by coupling this model with simple issues related to the mechanical properties of composite materials, it allows to determine the maximum possible gap between the electric dipoles in the dielectric inclusions. Therefore, the procedure described here could give a new mode for obtaining information about the spatial arrangement of dipoles in different kinds of composite dielectric materials.

Acknowledgments

This work was partially supported by the CONICET-PIP No. 179CO and 2098, the PID-UNR ING 450 and ING 453 (2014–2017). Dr. C. E. Boschetti and Dr. D. E. V. Giordano are acknowledged for providing the samples for present work and for assistance in preliminary measurements, respectively.

Appendix A

In order to obtain a value of the polarization of the molecule concentrated as a discrete dipole lying on the real molecular polarization axis, we will proceed as follows. Firstly, let us consider a two-dimensional projection of the dipolar sphere, Fig. 4(a), where we will take pairs of dipoles, of discrete charge q_e, symmetrically chosen (short dashed lines) regarding the real molecular polarization direction (dotted-dashed-line), Fig. A.1. In Fig. A.1, the case for only one pair of symmetric dipoles around the real polarization axis is shown for clarity. The resultant dipolar moment, p_{2D}, for the picture from Fig. A.1 can be written as

$$p_{2D} = 2\ 2r\ q\cos(\theta). \tag{A.1}$$

Subsequently, from a tri-dimensional analysis in the spherical dipolar molecule from Fig. A.2, the expression for the resultant differential dipolar moment by considering the projections over the real polarization molecular axis of both: (i) a pair of symmetric moments having a θ angle (regarding the real polarization axis) and (ii) a pair of symmetric moments having the azimuthal angle, φ, (regarding the real

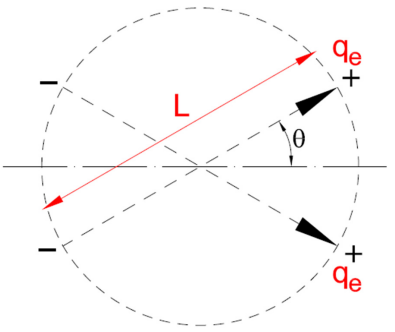

Fig. A.1. Two-dimensional projection of two symmetric dipoles of arbitrary charge, q_e, around the real molecular polarization direction.

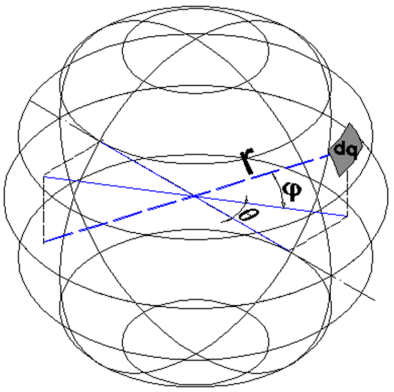

Fig. A.2. Three-dimensional angular configuration around the real molecular polarization direction for an arbitrary differential of charge, d_q.

polarization axis) takes the form;

$$dp_{3D} = 2 \cdot 2 \cdot 2r\, dq \cos(\theta) \cos(\varphi). \tag{A.2}$$

Consequently, from the point of view of the electrostatic of the continuous media, the resulting dipolar moment can be obtained from the integration of the superficial density of charge for the dipolar sphere, λp, between 0 and $\pi/2$ both for θ and φ, such that

$$p = 8r^3\lambda_d \int_0^{\frac{\pi}{2}} \cos(\theta) d\theta \int_0^{\frac{\pi}{2}} \cos(\varphi) d\varphi. \tag{A.3}$$

Then, the electrical dipolar moment for the sphere, p, equals

$$p = 8r^3\lambda_d. \tag{A.4}$$

By considering a density of charge like the ratio between a concentrated charge q and the half surface of the sphere, Eq. (A.4) can be written as

$$p = \frac{2}{\pi}(2rq). \tag{A.5}$$

It can be appreciated from Eq. (A.5) that the mismatch which appears for considering a dipolar representation with two concentrated charges, q, lying on the surface of the sphere, instead of the density of charge λ_d; is only a constant which equals $2/\pi$. Therefore, to make easier the study of the orientation processes among electrical dipoles in the dielectric liquid, the so-called average dipole representation will be introduced in the present work, see Fig. 5. Indeed, the dipolar spherical molecule will be considered as a single resulting dipole which concentrates on the two charges punctually in opposite points over the sphere diameter in the direction of the real molecular dipolar axis.

References

[1]R. R. Mocellini, O. A. Lambri, D. Gargicevich, F. G. Bonifacich, B. Weidenfeller, M. Anhalt and W. Riehemann, Magnetic memory effect in magnetite charged polypropylene composite, *Compos. Interf.* **24**, 611 (2017).

[2]T. Mura, *Micromechanics of Defects in Solids* (Martinus Nijhoff Publishers, New York, 1987).

[3]J. D. Eshelby, The determination of the elastic field of an ellipsoidal inclusion, and related problems, *Proc. Roy. Soc. London A* **241**, 376 (1957).

[4]O. A. Lambri, R. R. Mocellini, F. Tarditti, F. G. Bonifacich, D. Gargicevich, G. I. Zelada and C. E. Boschetti, Internal stresses in the electrostriction phenomenon viewed through dynamic mechanical analysis studies conducted under electric field, *IEEE Trans. Dielectr. Electr. Insul.* **21**, 2070 (2014).

[5]R. R. Mocellini, O. A. Lambri, F. G. Bonifacich, D. Gargicevich, F. Tarditti, M. Anhalt, B. Weidenfeller and W. Riehemann, Electro-rheological description of solids dielectrics exhibiting electrostriction, *IEEE Trans. Dielectr. Electr. Insul.* **23**, 2993 (2016).

[6]F. G. Bonifacich, E. D. V. Giordano, O. A. Lambri, D. Gargicevich, R. R. Mocellini, J. A. García, F. Plazaola, F. A. Sánchez, C. E. Boschetti and P. E. Salvatori, Study of dielectric strength in EPDM by nondestructive dynamic mechanical analysis in high electrical field, *IEEE Trans. Dielectr. Electr. Insul.*, **24**, 1840 (2017).

[7]O. A. Lambri, *A Review on the Problem of Measuring Non-Linear Damping and the Obtainment of Intrinsic Damping*, eds. D. Walgraef, J. Martínez-Mardones and C. H. Wörner, Chapter 5 (World Scientific Publishing Co. Pte. Ltd., Singapore, 2000), pp. 249–280.

[8]C. T. Wang, *Applied Elasticity* (McGraw-Hill, New York, 1953).

[9]E. J. Hearn, *Mechanics of Materials* (Pergamon Press, Oxford, 1995).

[10]J. I. Pérez-Landazábal, O. A. Lambri, F. G. Bonifacich, V. Sánchez-Alarcos, V. Recarte and F. Tarditti, Influence of defects on the irreversible phase transition in Fe–Pd ferromagnetic shape memory alloys, *Acta Mater.* **86**, 110 (2015).

[11]L. D. Landau and E. M. Lifshitz, *Classical Theory of the Fields* (Reverté, Barcelona, 1973).

[12]J. D. Jackson, *Classical Electrodynamics* (Alhambra, Madrid, 1980).

[13]R. R. Mocellini, O. A. Lambri, C. L. Matteo, J. A. García, G. I. Zelada-Lambri, P. A. Sorichetti, F. Plazaola, A. Rodríguez-Garraza and F. A. Sánchez, Elastic misfit in two-phase polymer, *Polymer* **50**, 4696 (2009).

[14]O. A. Lambri, F. Plazaola, E. Axpe, R. R. Mocellini, G. I. Zelada-Lambri, J. A. García, C. L. Matteo and P. A. Sorichetti, Modification of the mesoscopic structure in neutron irradiated EPDM viewed through positron annihilation spectroscopy and dynamic mechanical analysis, *Nucl. Inst. Meth. B* **269**, 336 (2011).

[15]A. H. Cottrell, *The Mechanical Properties of Matter* (John Wiley & Sons, Inc, New York, 1964).

[16]N. W. Tschoegl, *The Phenomenological Theory of Linear Viscoelastic Behaivour* (Springer-Verlag, Berlin, 1989).

[17]B. J. Lazan, *Damping of Materials and Members in Structural Mechanics* (Pergamon, London, 1968).

[18]C. Kittel, *Introduction to Solid State Physics* (John Wiley & Sons, New York, 1971).

[19]F. C. Brown, *The Physics of Solids* (W. A. Benjamin, INC, New York, 1967).

[20]J. A. Babor and J. Ibarz Aznárez, *Modern General Chemistry* (Marín, Barcelona, 1941).

[21]S. Ege, *Organic Chemistry, Structure and Reactivity* (Reverté, Barcelona, 1998).

[22]M. F. Ashby and D. R. Jones, *Engineering Materials, An Introduction to their Properties and Applications* (Pergamon Press, New York, 1980).
[23]I. M. Ward and J. Sweeney, *Mechanical Properties of Solid Polymers* (John Wiley & Sons, Chichester, 2012).
[24]J. D. Ferry, *Viscoelastic Properties of Polymers* (John Wiley & Sons, Inc., New York, 1980).
[25]R. R. Mocellini, O. A. Lambri, C. L. Matteo and P. A. Sorichetti, Dielectric properties and viscoelastic response in two-phase polymers, *IEEE Trans. Dielectr. Electr. Insul.* **15**, 982 (2008).